DOI: 10.1002/cmdc.200600115

Probing, Inhibition, and Crystallographic Characterization of Metallo-β-lactamase (IMP-1) with Fluorescent Agents Containing Dansyl and Thiol Groups

Hiromasa Kurosaki,*[a] Yoshihiro Yamaguchi,*[b] Hisami Yasuzawa,[a] Wanchun Jin,[a] Yuriko Yamagata,[c] and Yoshichika Arakawa[d]

The treatment of bacterial infections has advanced rapidly in recent years, primarily as the result of the development of multiple antibacterial agents.[1–3] However, with the widespread use of such antibacterial agents, various pathogens have developed a resistance to antibiotics and are now a global problem as nosocomial pathogens in immunocompromised patients.[4] One of the mechanisms of bacterial resistance is the production of enzymes that render drugs inactive.[5] For example, β-lactamases, produced by various pathogenic bacteria, catalyze the hydrolysis of the β-lactam ring of β-lactam antibiotics.[6–9]

β-Lactamases can be classified into four molecular classes: A, B, C, and D.[10,11] β-Lactamases in classes A, C, and D are serine enzymes with a serine residue at the active site, whereas class B β-lactamases require divalent metal ions such as Zn^{II}, and are referred to as the metallo-β-lactamases (MBLs).[6–9] MBLs are able to hydrolyze nearly all β-lactam antibiotics, including carbapenems, and are also generally not susceptible to β-lactamase inhibitors such as clavulanic acid, tazobactam, and sulbactam, which are routinely used for clinical treatment.[12]

Among the most widely recognized MBLs, IMP-1 is extremely widespread. The resistance gene, bla_{IMP}, is included in an integron structure that is present in the mobile plasmid as a cassette.[13] Therefore, it is possible for the gene to horizontally propagate to other bacteria, and the isolation of IMP-1 has been reported in both Japan and Europe.[14] The rampancy of pathogenic bacteria that retain IMP-1 is due to the fact that it efficiently hydrolyzes carbapenems, unlike the class A, C, and D β-lactamases. Thus, it is very important to confirm the production of IMP-1 in infectious bacteria for effective chemotherapy at the initial stages of a disease.

We are currently in the process of developing reagents for IMP-1 detection based on the use of a fluorescent probe. We recently reported that thiocarboxylic acid derivatives inhibit IMP-1, reversibly or irreversibly.[15–17] We have also reported on a fluorescent probe for detecting IMP-1, *N*-(5-(dimethylamino)-1-naphthalenesulfonamidoethyl)-3-thiopropionamide, (Dansyl-C_2SH, Figure 1).[18] A compound containing a thiol group as a

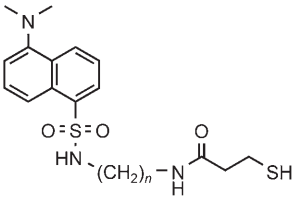

n = 2: DansylC_2SH; *n* = 3: DansylC_3SH;
n = 4: DansylC_4SH; *n* = 5: DansylC_5SH;
n = 6: DansylC_6SH

Figure 1. Structures of DansylC_nSHs (*n* = 2–6).

Zn^{II} ligand and a dansyl group as a fluorophore would be expected to serve as an effective fluorescent probe for detecting IMP-1. Moreover, in an attempt to optimize its fluorescence properties, we designed some new fluorescence probes, DansylC_nSHs (*n* = 2–6, Figure 1) in which the length of the methylene chain between the dansyl and thiol groups is varied.

Herein, we describe the synthesis, fluorescence properties, and inhibition activities of DansylC_nSHs with IMP-1. We also determined the X-ray crystal structure of IMP-1 complexed with DansylC_4SH, which, of the DansylC_nSHs examined to date, is the most highly sensitive fluorescent probe and an inhibitor of IMP-1. By connecting the dansyl and 3-thiopropionic acid groups with linkers of various length, the ability to detect and evaluate the inhibition activity of MBLs such as IMP-1,[13] VIM-2,[19] and variants thereof[20–23] can be tuned.

The fluorescent DansylC_nSH probes were synthesized in one-step reactions in 31–77% yield by condensing 3-thiopropionic acid with *N*-(aminoalkyl)-5-dimethylaminonaphthalene-1-sulfonamide using *N*,*N*′-dicyclohexylcarbodiimide followed by silica gel column chromatography (see Supporting Information).

We examined the ability of the fluorescent agent to detect IMP-1 by measurement of the fluorescence emission spectra ($\lambda_{excitation}$ = 340 nm) of 1 μM DansylC_nSHs with varying concentrations of IMP-1 (0–10 μM) in 50 mM Tris-HCl buffer (pH 7.4) containing 0.5 M NaCl and 10% methanol. As the concentration of IMP-1 increased, the fluorescence emission intensity of

[a] *Dr. H. Kurosaki, H. Yasuzawa, W. Jin*
Department of Structure–function Physical Chemistry
Graduate School of Pharmaceutical Sciences
Kumamoto University
Oe-honmachi 5-1, Kumamoto 862-0973 (Japan)
Fax: (+81) 96-371-4314
E-mail: ayasaya@gpo.kumamoto-u.ac.jp

[b] *Dr. Y. Yamaguchi*
Environmental Safety Center
Kumamoto University
39-1, Kurokami 2-Chome, Kumamoto 860-8555 (Japan)
Fax: (+81) 96-342-3238
E-mail: yyamagu@gpo.kumamoto-u.ac.jp

[c] *Prof. Dr. Y. Yamagata*
Department of Structural Biology
Graduate School of Pharmaceutical Sciences
Kumamoto University
Oe-honmachi 5-1, Kumamoto 862-0973 (Japan)

[d] *Director. Dr. MD Y. Arakawa*
Department of Bacterial Pathogenesis and Inflection Control
National Institute of Infectious Diseases
4-7-1 Gakuen, Musashi-Murayama, Tokyo 208-0011 (Japan)

Supporting information for this article is available on the WWW under http://www.chemmedchem.org or from the author.

the DansylC$_n$SHs also increased, and the fluorescence emission maxima were shifted to a shorter wavelength (Figure 2a–e), indicating that DansylC$_4$SH is the most blue-shifted amongst the DansylC$_n$SHs used in this study. At a concentration of 1 μM IMP-1, the ratios of the fluorescence intensities of 1 μM DansylC$_n$SHs in the presence and absence of 1 μM IMP-1 at $\lambda =$ 535 nm were 3.0 for $n=2$, 2.8 for $n=3$, 5.9 for $n=4$, 3.6 for $n=5$, and 3.5 for $n=6$.

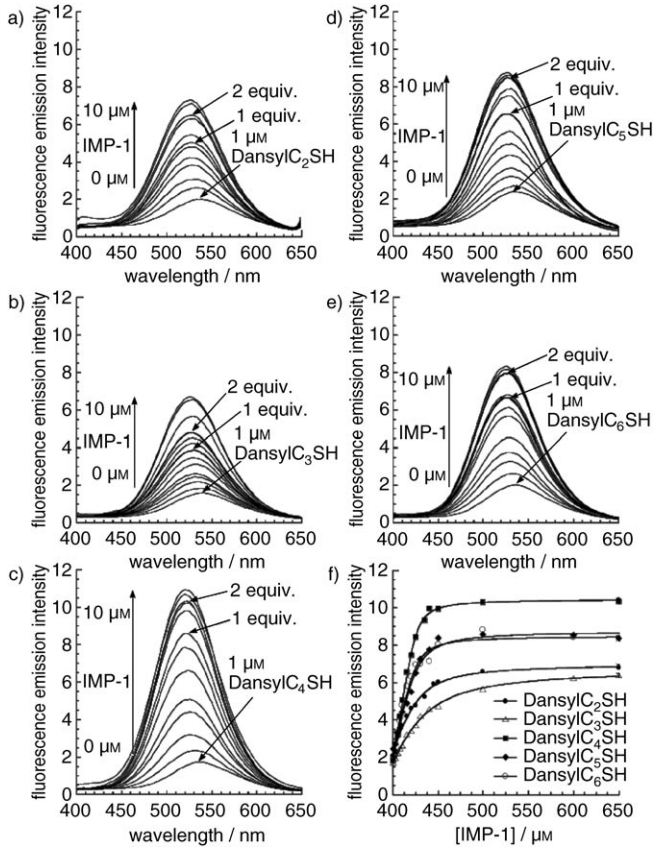

Figure 2. Fluorescence emission spectra ($\lambda_{excitation} = 340$ nm) of 1 μM DansylC$_n$SHs ($n=2$–6) with increasing concentrations of IMP-1 ranging from 0 to 10 μM: a) DansylC$_2$SH; b) DansylC$_3$SH; c) DansylC$_4$SH; d) DansylC$_5$SH; e) DansylC$_6$SH. These spectra were measured at 25 °C in 50 mM Tris-HCl buffer (pH 7.4) containing 0.5 M NaCl and 10% methanol. f) Fluorescence emission intensity as a function of the concentration of added IMP-1 monitored at $\lambda = 535$ nm. The apparent dissociation constants of each DansylC$_n$SH with IMP-1 were analyzed from the data by nonlinear least-squares fitting using Equation (5) in the Supporting Information.

When changes in the fluorescence emission intensity at $\lambda =$ 535 nm were plotted as a function of the concentration of IMP-1, a plateau was observed for concentrations of IMP-1 above 1 μM (Figure 2f). The apparent dissociation constants (K_d) of DansylC$_n$SHs with IMP-1 were estimated by nonlinear least-squares fitting of the titration data. The calculated K_d values were in the range of 67–975 nM (Table 1), indicating that DansylC$_4$SH binds to IMP-1 more tightly than the other DansylC$_n$SHs (for example, about 15-fold greater than DansylC$_3$SH). As determined from the dependence of the concentration of IMP-1 on the fluorescence emission intensity, all of the DansylC$_n$SHs bind to IMP-1 to form a 1:1 complex.

Table 1. Dissociation and inhibition constants and IC_{50} values for DansylC$_n$SHs ($n=2$–6) toward IMP-1.

Compd	K_d [nM][a]	K_i [nM][b]	IC_{50} [μM][b]
DansylC$_2$SH	356 ± 66	1100 ± 60	5.2 ± 0.4
DansylC$_3$SH	975 ± 110	1300 ± 100	6.3 ± 0.7
DansylC$_4$SH	67 ± 14	140 ± 10	0.7 ± 0.1
DansylC$_5$SH	154 ± 41	280 ± 10	1.6 ± 0.1
DansylC$_6$SH	105 ± 42	160 ± 10	1.0 ± 0.1

[a] Determined at 25 °C; for details, see Supporting Information. [b] Determined at 30 °C; for details, see Supporting Information.

Previously, we reported that DansylC$_2$SH did not cause fluorescence enhancement in the presence of carbonic anhydrase, which contains a zinc(II) ion in the active site.[18] This fluorescence enhancement was also not observed with other DansylC$_n$SHs ($n=4$–6).

Considering the clinical applications of DansylC$_n$SHs, one of the major problems is whether DansylC$_n$SHs can be used to detect other MBLs. Therefore, we measured the fluorescence spectra of DansylC$_n$SHs in the presence of VIM-2. VIM-2, like IMP-1, is also extremely widespread. Although carbapenemase-producing organisms are rare in the United States, a nosocomial outbreak of pan-resistant *Pseudomonas aeruginosa* was reported recently;[24] the strain expressed an integron-borne VIM-2. The Trp64 residue located at the top of loop 1 in IMP-1 is replaced by an alanine residue in VIM-2. This mutation is predicted to cause the fluorescence emission intensity to have different characteristics. Similar to IMP-1, the fluorescence emission intensity of DansylC$_n$SH increased with increasing concentrations of VIM-2 (see Supporting Information). However, the fluorescence intensity increases with the number of the methylene groups in the linker (i.e. DansylC$_6$SH showed a maximal fluorescence enhancement, with a K_d value of 190 nM; see Supporting Information). These results suggest that Trp64 in IMP-1 is an important factor in controlling the fluorescence properties of DansylC$_n$SH with MBLs.

We screened for inhibitory activity against IMP-1 from *Serratia marcescens* by measuring the initial velocity (v_i) against nitrocefin as a substrate in the presence of several concentrations of DansylC$_n$SHs. IC_{50} (half-maximal inhibition) values were determined from a plot of fractional activity remaining against the concentration of DansylC$_n$SH (see Supporting Information). Moreover, the inhibition constant (K_i) for each DansylC$_n$SH was calculated according to a competitive inhibition pattern by fitting the kinetic data (see Supporting Information). The IC_{50} and K_i values for IMP-1 were calculated to be 0.7–6.3 μM and 140–1300 nM, respectively. These results imply that the most potent inhibitor of IMP-1 was DansylC$_4$SH. In the case of VIM-2, the IC_{50} and K_i values were calculated to be 1.5–3.4 μM and 286–720 nM, respectively (see Supporting Information).

The question of why DansylC$_4$SH exhibits the most fluorescence enhancement and inhibition among DansylC$_n$SHs is of interest. To address this, we prepared co-crystals of DansylC$_4$SH and IMP-1 to carry out an X-ray crystallographic analysis. The

X-ray crystal structure of the DansylC$_4$SH–IMP-1 complex was determined at a resolution of 2.43 Å by molecular replacement using the coordinates of IMP-1 (PDB code 1DD6).[25] There were two molecules in an asymmetric unit, denoted as molecules A and B. The structure of the complex was refined to a final $R_{working}$ value of 18.5% and an R_{free} value of 22.4% for data from 19.8 to 2.43 Å.[26] Superposition of the α-carbon atoms of the two independent molecules A and B in the asymmetric unit gave a root-mean-square deviation (rmsd) of 0.35 Å.

The overall structure of each molecule adopts an αβ/βα sandwich structure, as is also found in native IMP-1 (Figure 3a).

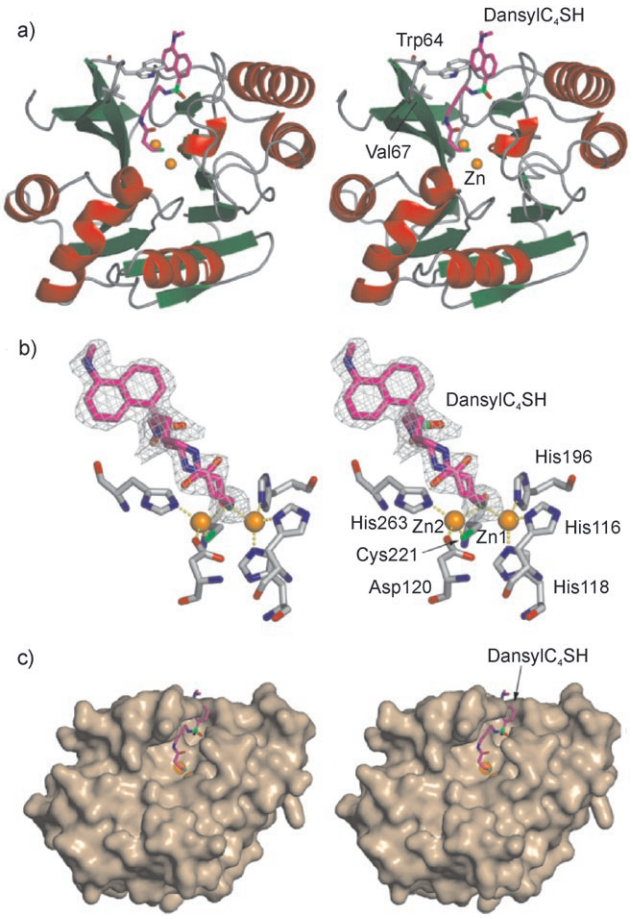

Figure 3. a) Overall structure of IMP-1 complexed with DansylC$_4$SH. DansylC$_4$SH has alternate conformations (Figure 3b) but herein, only one is represented. α Helices, β strands, and loops are shown in red, green, and gray, respectively. Zn^{II} atoms are shown as orange spheres. Carbon atoms in the DansylC$_4$SH are shown in violet. Trp64 and Val67 residues and DansylC$_4$SH are represented as sticks. Carbon atoms in Trp64 and Val67 residues are shown in gray (nitrogen = blue; oxygen = red; and sulfur = light green). b) The structure of the active site of IMP-1 complexed with DansylC$_4$SH. The electron density map (gray) of DansylC$_4$SH is shown contoured at the 2.5σ level in the F_o-F_c map. Zn^{II} atoms are shown as orange spheres. Carbon atoms of DansylC$_4$SH are shown in violet. His116, His118, His196, His263, Asp120, and Cys221 residues and DansylC$_4$SH are represented as sticks. Carbon atoms in His116, His118, His196, His263, Asp120, and Cys221 residues are shown in gray (nitrogen = blue; oxygen = red; and sulfur = light green). c) Molecular surface representation[32] of IMP-1 complexed with DansylC$_4$SH. Zn^{II} atoms are shown as orange spheres. Carbon, nitrogen, oxygen, and sulfur atoms of DansylC$_4$SH are shown in violet, blue, red, and light green, respectively.

The DansylC$_4$SH–IMP-1 complex and native IMP-1 (PDB code 1DDK)[25] were also superimposed, except for residues 62–65 which were disordered in native IMP-1, and the rmsd for C^α between the complex and native IMP-1 was 0.52 Å for molecule A and 0.54 Å for molecule B. Glu60, Val61, and Val66, positioned on the base of a hairpin loop (residues 61–66, loop 1), confer flexibility near the active site. Asn185 is positioned in the other loop, which is exposed to solvent, and Asn233 and Gly235 are located in another loop (residues 221–241, loop 2) near the active site.

The active site of the DansylC$_4$SH–IMP-1 complex is shown in Figure 3b. As seen in the F_o-F_c electron density map, a portion clearly alternates in the crystal and the two conformations fit the map very well, with the exception of the sulfonamide group of the naphthyl ring and the terminal thiol group in DansylC$_4$SH. Therefore, the corresponding atoms in the two conformations were refined with an occupancy of 0.5 in each case. The thiol group sulfur atom in DansylC$_4$SH bridges to two Zn^{II} ions (Zn1 and Zn2) with Zn1–S distances of 2.1 and 2.4 Å in molecules A and B, respectively, and with Zn2–S distances of 2.4 and 2.3 Å, respectively. Among the dinuclear Zn^{II} MBLs, a bridging H_2O or OH^- between Zn1 and Zn2 is thought to act as the attacking nucleophile on the carbonyl carbon atom of the β-lactam ring.[27–29] The bridging H_2O or OH^- would be replaced with a sulfur atom of the thiol group in DansylC$_4$SH in the complex. This Zn^{II} coordination geometry is tetrahedral at both sites. On the other hand, in the case of native IMP-1, the coordination environment for the Zn2 site is proposed to have a disordered trigonal bipyramidal geometry occupied by a bridging H_2O or OH^-, Cys221, and His263 in the equatorial positions, whereas Asp120 and the second H_2O occupy apical positions.[25] The second H_2O is thought to contribute to the catalysis of the hydrolysis of β-lactams.[30,31] It is proposed that the bridging of a thiol group to two Zn^{II} ions not only replaces a bridging H_2O or OH^- but also prevents H_2O from coordinating to the Zn2 site.

The naphthyl ring of DansylC$_4$SH is stabilized by a CH–π interaction (edge-to-face) with the indole ring of the Trp64 residue, leading to a change in the conformation of Trp64. The three-dimensional structure of IMP-1 complexed with the thiocarboxylate inhibitor 2-(5-(1-tetrazoylmethyl)thien-3-yl)-*N*-(2-(thiomethyl)-4-(phenylbutyrylglycine)) has also been reported to have a similar interaction.[25] In addition, the remaining portions between the naphthyl ring and a thiol group make hydrophobic contact with the Val61 residue (Figure 3a) and cover the shallow and wide active site cavity (Figure 3c).

Among the DansylC$_n$SHs, DansylC$_4$SH has an optimum length for binding to two Zn^{II} ions, replacing the bridging H_2O or OH^- that act as nucleophiles and the edge-to-face interaction with Trp64. The weakness of interaction between IMP-1 and other DansylC$_n$SHs may be due to steric hindrance or a lack of an attractive interaction between the enzyme, but further investigations for elucidating the relationships between structural and fluorescence properties are needed.

In conclusion, a series of dansyl derivatives, DansylC$_n$SHs (n = 2–6), derived from *N*-(aminoalkyl)-5-dimethylaminonaphthalene-1-sulfonamide and 3-thiopropionic acid, were synthe-

sized in an attempt to develop a fluorescent probe for the detection of MBLs. DansylC_nSHs act not only as fluorescent probes, but also as inhibitors of IMP-1 and VIM-2. The three-dimensional structure of IMP-1 complexed with DansylC_4SH was determined; the main interactions occur between the naphthyl ring of the DansylC_4SH and Trp 64 with an edge-to-face interaction, and the thiol group is coordinated to two Zn^{II} ions. These conclusions are also supported by fluorescence spectroscopy data. Thus, the spectral and structural data support the validity of our design strategy, which is aimed at developing both detection agents and inhibitors of MBLs. Finally, we expect that the fluorescent probes investigated in this study will serve as lead compounds for the further development of detection agents and specific high-affinity inhibitors that are selective for MBLs.

Acknowledgements

Work related to the preparation, purification, and inhibition studies of the enzymes was supported by a Grant from the Ministry of Health, Labor, and Welfare of Japan (H15-Shinkou-9). The synthetic, spectroscopic, and X-ray crystallographic studies were supported by a Grant-in-Aid for Scientific Research (B) (No. 16390017) from the Japanese Society for the Promotion of Science.

Keywords: bioinorganic chemistry · crystal structure analysis · fluorescent probes · inhibitors · metalloenzymes

[1] K. Bush, M. Macielag, M. Weidner-Wells, *Curr. Opin. Microbiol.* **2004**, *7*, 466 – 476.
[2] C. J. Thomson, E. Power, H. Ruebsamen-Waigmann, H. Labischinski, *Curr. Opin. Microbiol.* **2004**, *7*, 445 – 450.
[3] D. Payne, A. Tomasz, *Curr. Opin. Microbiol.* **2004**, *7*, 435 – 438.
[4] F. M. Walsh, S. G. Amyes, *Curr. Opin. Microbiol.* **2004**, *7*, 439 – 444.
[5] J. M. Thomson, R. A. Bonomo, *Curr. Opin. Microbiol.* **2005**, *8*, 518 – 524.
[6] U. Heinz, H. W. Adolph, *Cell. Mol. Life Sci.* **2004**, *61*, 2827 – 2839.
[7] M. S. Helfand, R. A. Bonomo, *Curr. Opin. Pharmacol.* **2005**, *5*, 452 – 458.
[8] J. F. Fisher, S. O. Meroueh, S. Mobashery, *Chem. Rev.* **2005**, *105*, 395 – 424.
[9] T. R. Walsh, M. A. Toleman, L. Poirel, P. Nordmann, *Clin. Microbiol. Rev.* **2005**, *18*, 306 – 325.
[10] R. P. Ambler, *Philos. Trans. R. Soc. London Ser. B* **1980**, 289, 321 – 331.
[11] M. Galleni, J. Lamotte-Brasseur, G. M. Rossolini, J. Spencer, O. Dideberg, J.-M. Frère, *Antimicrob. Agents Chemother.* **2001**, *45*, 660 – 663.
[12] K. Bush, G. A. Jacoby, A. A. Medeiros, *Antimicrob. Agents Chemother.* **1995**, *39*, 1211 – 1233.
[13] Y. Arakawa, M. Murakami, K. Suzuki, H. Ito, R. Wacharotayankun, S. Ohsuka, N. Kato, M. Ohta, *Antimicrob. Agents Chemother.* **1995**, *39*, 1612 – 1615.
[14] G. Cornaglia, M. L. Riccio, A. Mazzariol, L. Lauretti, R. Fontana, G. M. Rossolini, *Lancet* **1999**, *353*, 899 – 900.
[15] J. Spencer, T. R. Walsh, *Angew. Chem.* **2006**, *118*, 1038 – 1042; *Angew. Chem. Int. Ed.* **2006**, *45*, 1022 – 1026.
[16] M. Goto, T. Takahashi, F. Yamashita, A. Koreeda, H. Mori, M. Ohta, Y. Arakawa, *Biol. Pharm. Bull.* **1997**, *20*, 1136 – 1140.
[17] H. Kurosaki, Y. Yamaguchi, T. Higashi, K. Soga, S. Matsueda, H. Yumoto, S. Misumi, Y. Yamagata, Y. Arakawa, M. Goto, *Angew. Chem.* **2005**, *117*, 3929 – 3932; *Angew. Chem. Int. Ed.* **2005**, *44*, 3861 – 3864.
[18] H. Kurosaki, H. Yasuzawa, Y. Yamaguchi, W. Jin, Y. Arakawa, M. Goto, *Org. Biomol. Chem.* **2003**, *1*, 17 – 20.
[19] L. Poirel, T. Naas, D. Nicolas, L. Collet, S. Bellais, J.-D. Cavallo, P. Nordmann, *Antimicrob. Agents Chemother.* **2000**, *44*, 891 – 897.
[20] J.-J. Yan, W.-C. Ko, J.-J. Wu, *Antimicrob. Agents Chemother.* **2001**, *45*, 2368 – 2371.
[21] M. L. Riccio, N. Franceschini, L. Boschi, B. Caravelli, G. Cornaglia, R. Fontana, G. Amicosante, G. M. Rossolini, *Antimicrob. Agents Chemother.* **2000**, *44*, 1229 – 1235.
[22] S. Iyobe, H. Kusadokoro, J. Ozaki, N. Matsumura, S. Minami, S. Haruta, T. Sawai, K. O'Hara, *Antimicrob. Agents Chemother.* **2000**, *44*, 2023 – 2027.
[23] Y.-W. Chu, M. Afzal-Shah, E. T. S. Houang, M.-F. I. Palepou, D. J. Lyon, N. Woodford, D. M. Livermore, *Antimicrob. Agents Chemother.* **2001**, *45*, 710 – 714.
[24] K. Lolans, A. M. Queenan, K. Bush, A. Sahud, J. P. Quinn, *Antimicrob. Agents Chemother.* **2005**, *49*, 3538 – 3540.
[25] N. O. Concha, C. A. Janson, P. Rowling, S. Pearson, C. A. Cheever, B. P. Clarke, C. Lewis, M. Galleni, J.-M. Frère, D. J. Payne, J. H. Bateson, S. S. Abdel-Meguid, *Biochemistry* **2000**, *39*, 4288 – 4298.
[26] The atomic coordinates of IMP-1, when complexed with DasylC4SH have been deposited in the Protein Data Bank with the following accession code: 2DOO.
[27] N. O. Concha, B. A. Rasmussen, K. Bush, O. Herzberg, *Structure* **1996**, *4*, 823 – 836.
[28] J. H. Ullah, T. R. Walsh, I. A. Taylor, D. C. Emery, C. S. Verma, S. J. Gamblin, J. Spencer, *J. Mol. Biol.* **1998**, *284*, 125 – 136.
[29] Z. Wang, W. Fast, A. M. Valentine, S. J. Benkovic, *Curr. Opin. Chem. Biol.* **1999**, *3*, 614 – 622.
[30] M. P. Yanchak, R. A. Taylor, M. W. Crowder, *Biochemistry* **2000**, *39*, 11 330 – 11 339.
[31] J. D. Garrity, A. L. Carenbauer, L. R. Herron, M. W. Crowder, *J. Biol. Chem.* **2004**, *279*, 920 – 927.
[32] A. Nicholls, GRASP, Graphical Representation and Analysis of Surface Properties, Columbia University, New York, **1992**.

Received: May 6, 2006
Published online on August 28, 2006

